Available online at www.sciencedirect.com
SCIENCE DIRECT®
Sensors and Actuators B 102 (2004) 117–125
SENSORS AND ACTUATORS B CHEMICAL
www.elsevier.com/locate/snb

Micromachined nanocrystalline SnO_2 chemical gas sensors for electronic nose

Jianwei Gong [a], Quanfang Chen [a,*], Weifeng Fei [b], Sudipta Seal [b]

[a] *Department of Mechanical, Material & Aerospace Engineering, University of Central Florida, Orlando, FL 32826, USA*
[b] *Advanced Materials Processing and Analysis Center (AMPAC), University of Central Florida, Orlando, FL 32826, USA*

Received 31 July 2003; received in revised form 23 February 2004; accepted 26 February 2004

Available online 15 June 2004

Abstract

MEMS-based batch fabrication compatible sol–gel synthesized mesoporous nanocrystalline SnO_2 gas sensor has been developed. The SnO_2 nanofilm is fabricated with the combination of polymeric sol–gel chemistry and block copolymers used as structure directing agents. The novel hydrogen sensor has a fast response time (2 s) and quick recovery time (10 s), as well as good sensitivity (up to 90), in comparing to other hydrogen sensors developed. The working temperature of the sensor developed can be reduced as low as 100 °C. The low working temperature poses advantages such as lower power consumption; lower thermal induced signal shift as well as safe detection in certain environments where temperature is strictly limited. The nanocrystalline SnO_2 sensor has a broad sensitivity. The developed sensor cell will be used to develop a high sensitivity and high selectivity electronic nose for harmful chemical gas detection by combining different catalysts doped SnO_2 gas sensor array with fuzzy neural network.

Keywords: MEMS; Nanocrystalline SMO; Sol–gel; Electronic nose

1. Introduction

There is no single gas sensor existing that is 100% selective to a single chemical gas [1]. Therefore, a gas sensor array able to detect different interested gases has been a major focus of research on gas sensors for years. Electronic nose, a system of a sensor array, has a wide range of potential applications such as air quality control in HVAC system, safety/anti-terrorism, explosive gas (bomb) and hazardous pollutant gas detection in public area like airport, shopping center, etc. [1–5]. Other areas include odors detection in industries including food, drink, chemical, etc. applications in automobile and space, smart domestic applications and health cares [6–12]. Deploying analytical systems such as Fourier transform infrared (FTIR) and gas chromatographs and mass spectrometers have certain difficulties, namely: requirement of skilled and knowledgeable operators, very expensive of the facility and high maintenance cost, slow response time, and large size that is difficult for site monitoring. A desirable gas detection system can be described as followings: portable and corrosion resistant that is capable of being installed in hazardous areas, durable and operationally stable, simple and minimum needs in maintenance, enable for a minimally skilled person to operate and cost effective [1].

In the past a few decades, semiconductor metal oxide (SMO) gas sensors have emerged as efficient gas detection tools [13–15]. Compared to other gas sensing techniques such as conductive polymer, oscillating (QMB, BAW, and SAW), electrochemical cell and fiber optical, SMO gas sensors have advantages, such as more robust (up to 10-year-life time), less sensitive to environmental moisture and temperature, simple interface electronics, faster response time and fast recovery time [9,13–16]. In addition, a single SMO sensor has broader sensitivity than any other sensing technologies. The sufficient selectivity can be achieved by placing several doped sensors together into an array. In this case, the broad sensitivities of SMO to different gases can be turned into an advantages [16] as a smaller number of sensing cells are needed in the array. MEMS-based SMO gas sensor can be fabricated using IC compatible processes, which means low cost due to batch microfabrication. Therefore, SMO gas sensor may represent the best sensing cells for chemical gas sensing electronic nose development.In this research, mesoporous nanocrystalline tin oxide thin film has been fabricated using polymeric sol–gel process together with block copolymer

* Corresponding author. Tel.: +1-407-823-2152; fax: +1-407-823 0208.
E-mail address: qchen@mail.ucf.edu (Q. Chen).

0925-4005/$ – see front matter © 2004 Elsevier B.V. All rights reserved.
doi:10.1016/j.snb.2004.02.055

structure-directing method. MEMS-based gas sensor cell with such gas sensing film was fabricated and tested. Fast response (1 s) and quick recovery time (3 s) and good sensibility to hydrogen have been achieved. The developed sensor cell will be used to develop a high sensitivity and high selectivity electronic nose for harmful gas detection by combining different catalysts doped SnO_2 gas sensor array with fuzzy neural network.

2. Experimental

2.1. Gas sensor design and fabrication

The MEMS-based gas sensor cell is sketched in Fig. 1, and the fabrication process is shown in Fig. 2. Alumina wafer was used as substrate for better thermal and electrical isolation purposes. Pt micro heater and temperature sensor underneath the sensing cell was fabricated by a thermal deposition and lift off process. Then, a high dielectric spin-on glass was spin coated on top as the electric isolation layer. Gas sensing thin film was fabricated by spin coating of a prepared sol and a calcinning process. The sensing electrode was then deposited by a thermal evaporation and patterned by liftoff (Fig. 3).

2.2. Preparation of sol

Porous nanocrystalline tin oxide layer was developed by polymeric sol–gel technique. A precursor of tin isopropoxide ($Sn(O^iPr)_4$, 10%, alfa aesar) 25 ml, 5 ml deionized water were firstly dissolved in 50 ml anhydrous ethanol followed by magnetic stirring for half-an hour. Then a complexing agent, acetylacetone (AcAc) 3 ml was added to stabilize the hydrolysis of tin isopropoxide.

After completely mixing using magnetic stirring for 2 h, a 10 wt.% triblock copolymer Pluronic F127 (PEO–PPO–PEO) was dissolved into the solution [19,20], this solution

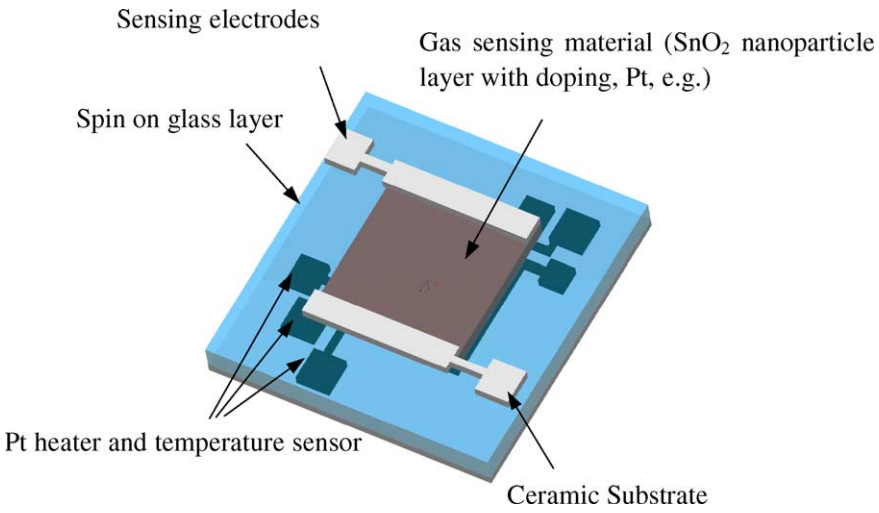

Fig. 1. Single SnO_2 gas sensor cell.

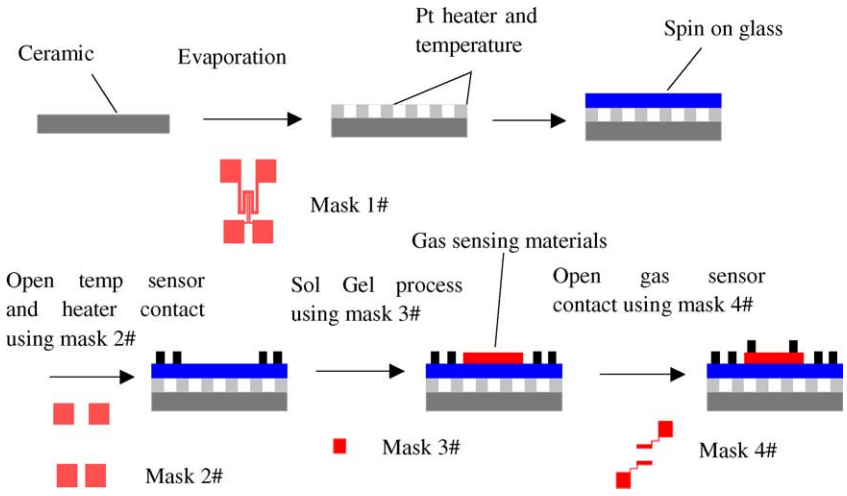

Fig. 2. Fabrication process of gas sensor cell.

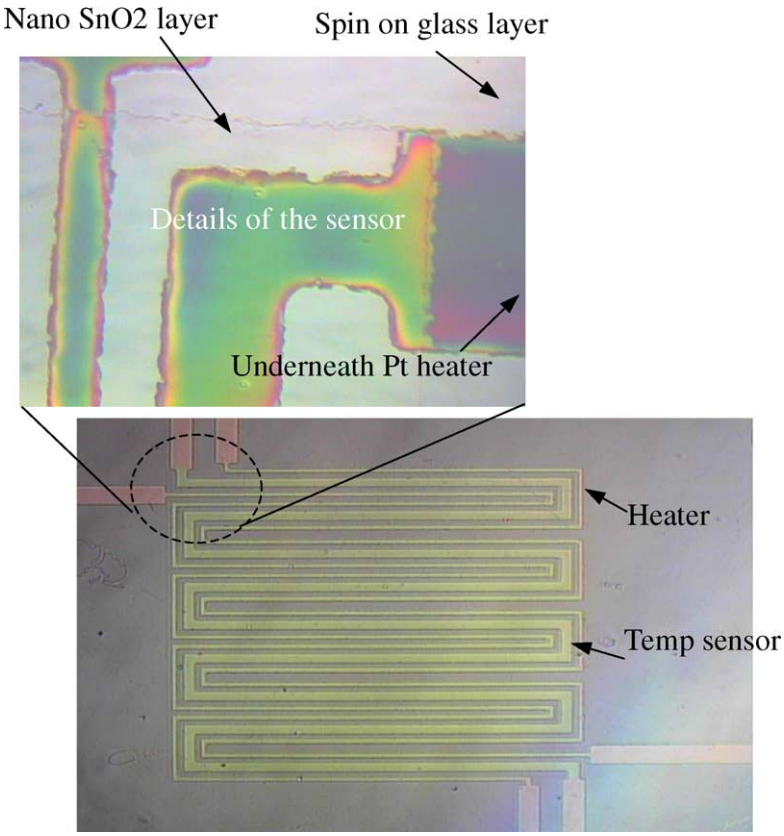

Fig. 3. Microscopic picture of a fabricated device.

was put on hotplate at 50 °C, stirring for 2 days. The viscosity of the sol was adjusted with addition of PVA (polyvinyl alcohol). Then, this prepared sol will be filtered seven times before usage.

2.3. SnO_2 thin film fabrication by sol–gel process

Nanostructured SnO_2 thin film was fabricated by a spin coating together with a subsequent calcinning process. A ramp spin coating method was used to increase spinning speed gradually up to 5000 rpm and keep spinning for 30 s total. After air-dry the film for 1 min, this film was ready for another round of spin coating and air-dry if multiple coating is needed to increase the thickness. The coated film was dried in an oven at 100 °C for 30 min. The film calcinning was conducted in a furnace (thermolyne) with a heating rate of 2 °C/min incensement to 500 °C and kept it at this temperature for 2 h. The thickness of SnO_2 film was measured by Tencor® profile meter. The measured thickness is about 150 nm with single spin coating at 5000 rpm spinning speed. Fig. 4 shows that mesoporous structures of nano SnO_2 particles after calcinning, and Fig. 5 shows the cross section of a film coated six times on purpose to achieve a thicker film for better viewing.

2.4. Dopants and catalysts

Sol–gel synthesis method allows easy manipulations of adding doping material to achieve the selectivity with atomic level mixing and uniform dispersion efficiency. For the H_2 detection purposes, silver (Ag) and platinum (Pt) have been added as doping material in SnO_2 to achieve better sensitivity and selectivity on H_2 during this research. For the Ag doping that $AgNO_3$ was added into the SnO_2 sol and followed by a magnetic stirring (for 24 h), while HNO_3 was used to stabilize the SnO_2 sol. The catalyst metal Pt was introduced by a sputtering process. After SnO_2 thin film was spin coated and calcined, Pt was sputtered onto the surface of SnO_2 thin film followed by a thermal diffusion process.

2.5. Experimental procedures

The testing system consists H_2 and pure air gas cylinders with regulators (airgas), a 2 cm^3/min mass flow controller (omega), flow meters, a gas chamber, and oscilloscope (TDS 224) together with National Instrument Data Acquisition System. The chamber was firstly purged completely with pure air, and hydrogen gas was introduced into the chamber to achieve the desired concentration by the mass flow controller, the concentration range of hydrogen is

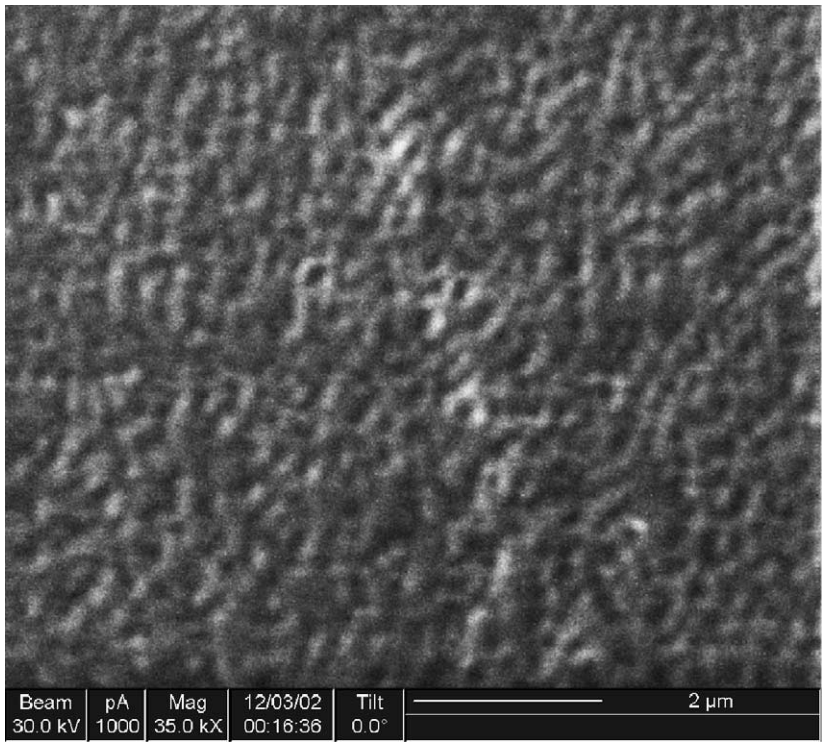

Fig. 4. Porous structure of SnO_2 nanosize film developed under SEM.

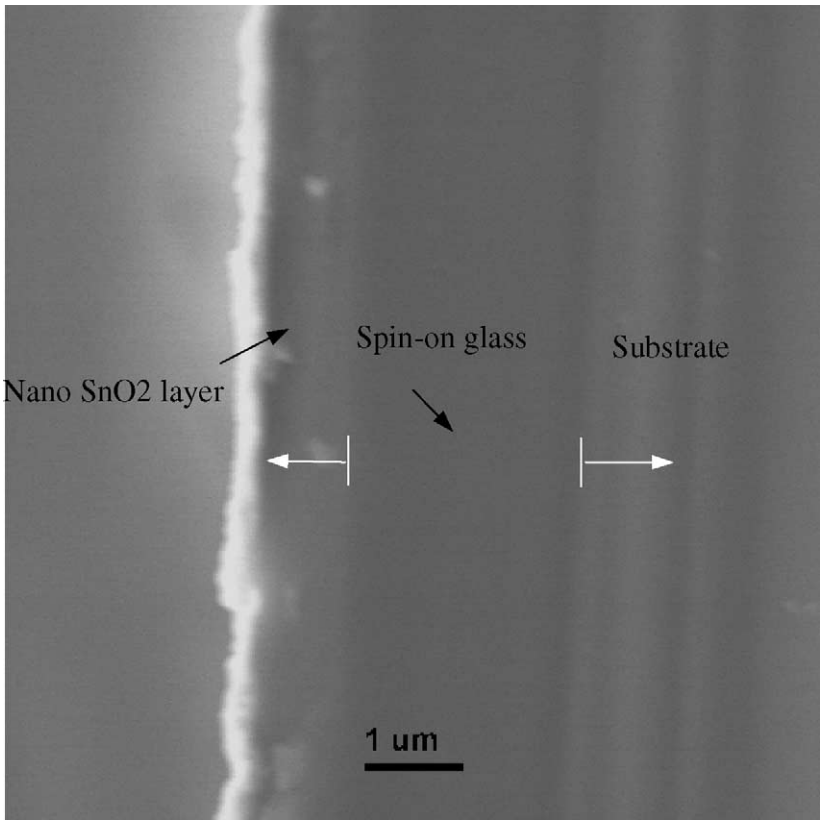

Fig. 5. SEM picture shown cross-section and thickness of nanofilm and the spin-on glass film.

from 1000 ppm to 10,000 ppm (1%) Then, pure air is introduced again for gas sensor recovery. The sensitivity was determined by:

$$\text{sensitivity} = \frac{R_1 - R_0}{100 R_0}$$

where R_1 is resistance values of gas sensing thin film in air, and R_0 represents resistance values in gas environment.

Fabricated gas sensors, both a sensing cell with SnO_2 + Pt thin film and a gas sensor cell with SnO_2 + Ag + Pt thin film, were tested in the above-mentioned concentration of hydrogen environment. The sensibility test of the fabricated undoped SnO_2 nanofilm sensors to other chemicals, such as hydrocarbons including acetone and ethanol, were tested also during the study.

3. Result and discussion

Test results of fabricated SnO_2 + Pt thin film gas sensor cell and SnO_2+Pt+Ag thin film gas sensor cell in a series of hydrogen concentration environment and different working temperatures are presented in Figs. 6–11. The comparison of gas sensing performance for these two types of sensors are summarized in Tables 1–3. The results shows that SnO_2/Pt/5%Ag film has achieved better sensing results than

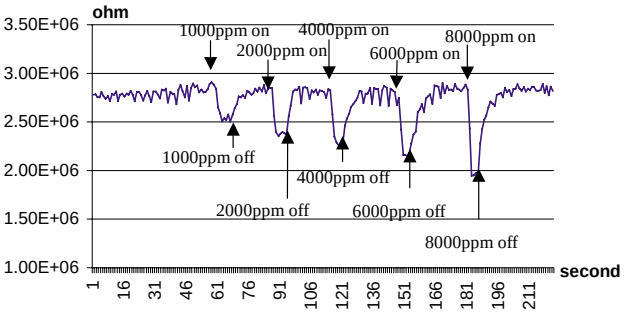

Fig. 8. Response of SnO_2 + sputtered Pt to H_2 at 200 °C.

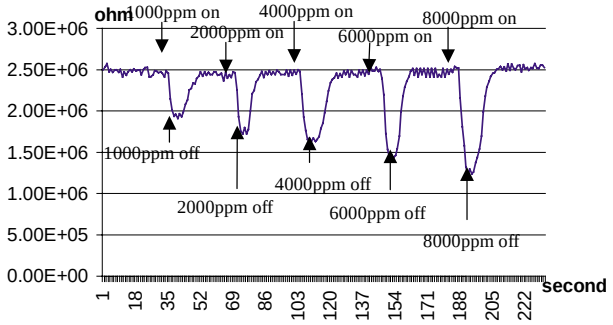

Fig. 9. Response of SnO_2 + 5% Ag + sputtered Pt to H_2 at 200 °C.

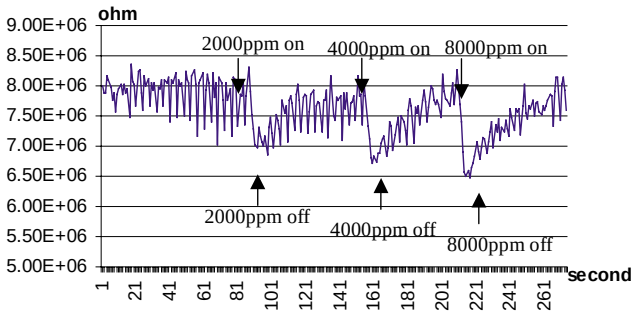

Fig. 6. Response of SnO_2 + 5% Ag + sputtered Pt to H_2 at 100 °C.

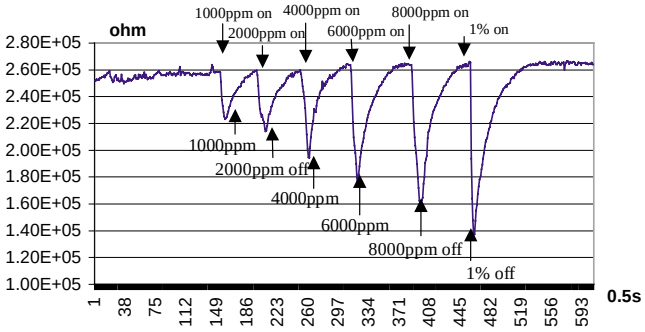

Fig. 10. Response of SnO_2 + sputtered Pt H_2 250 °C.

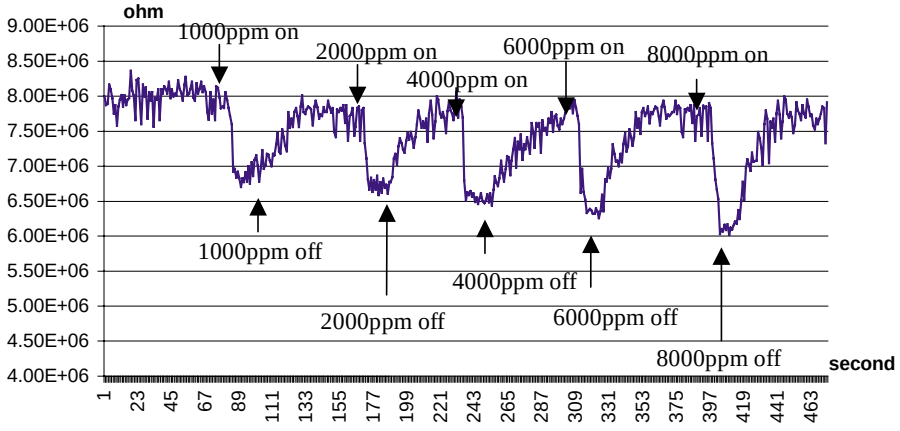

Fig. 7. Response of SnO_2 + 5% Ag + sputtered Pt to H_2 at 100 °C.

Table 1
Comparison of sensitivity to hydrogen at 100 °C

	2000 ppm	4000 ppm	8000 ppm	Response time (s)	Recovery time (s)
SnO_2/Pt	14[a]	18[a]	23[a]	~6	~40
SnO_2/5% Ag/Pt	17[a]	23[a]	30[a]	~5	~40

[a] Values given in percentage.

Table 2
Comparison of sensitivity to hydrogen at 200 °C

	1000 ppm	2000 ppm	4000 ppm	6000 ppm	8000 ppm	Response time (s)	Recovery time (s)
SnO_2/Pt	15[a]	20[a]	24[a]	31[a]	40[a]	~4	~20
SnO_2/5% Ag/Pt	24[a]	38[a]	53[a]	70[a]	90[a]	~4	~15

[a] Values given in percentage.

Table 3
Comparison of sensitivity to hydrogen at 250 °C

	1000 ppm	2000 ppm	4000 ppm	6000 ppm	8000 ppm	1%	Response time (s)	Recovery time (s)
SnO_2/Pt	18[a]	22[a]	30[a]	44[a]	63[a]	85[a]	~2	~20
SnO_2/5% Ag/Pt	30[a]	41[a]	53[a]	64[a]	79[a]	100[a]	~2	~10

[a] Values given in percentage.

SnO_2 + Pt sensing film. We can observe that SnO_2/Pt/5%Ag film has less baseline drift, better sensibility, faster response time and quicker recovery time in comparing to SnO_2/Pt film. The doped Ag could improve the sensing ability of SnO_2 thin film to hydrogen. It also indicates that for both thin film gas sensors, a fairly good sensitivity can be achieved at 100 °C. Better results have been achieved at higher temperatures such as 200 and 250 °C. Another characterization of both sensors is the fast response time (2–6 s) and quick recovery time (10–40 s) to hydrogen compared to other reported H_2 gas sensors. For example, Miremadi and Colbow reported 15–30 s response time and 20–60 s recovery time of single layer carbon film to 10^3 ppm H_2 [21]. Arya et al. reported several second's response time of ZnO + Pd thin film to H_2 [22], Hyodo et al. reported response time of 14–21 s and a recovery time of up to 35 min of nanosized mesoporous powder SnO_2 paste to H_2 [23], and other researchers reported longer response time and recovery time [24–29].

The sensors using pure SnO_2 film have also fabricated by sol–gel without doping and have been tested to detect hydrocarbons. The tested results to acetone and ethanol at 300 °C are shown in Figs. 12 and 13. A comparison of sensitivity, response time and recovery time to acetone and ethanol at 300 °C is shown in Table 4. We can see from Table 4 that even though there are no catalysts doped, the fabricated SnO_2 nanofilms have good sensitivity, quick response time and recovery time. Better selectivity can be achieved by combing proper working temperature scheme and doping scheme, algorithm like artificial neural network (ANN) should be used for data processing.

The gas detection principle of semiconductor type gas sensor is based on variations of the depletion layer at the grain boundaries in presence of reducing or oxidation gases which lead to variation in the height of the energy barriers for free charge carriers (e.g. electrons in SnO_2) [17]. When particle size decreases, the surface to volume ratio increase largely (reverse proportional to the particle size). The enhanced sen-

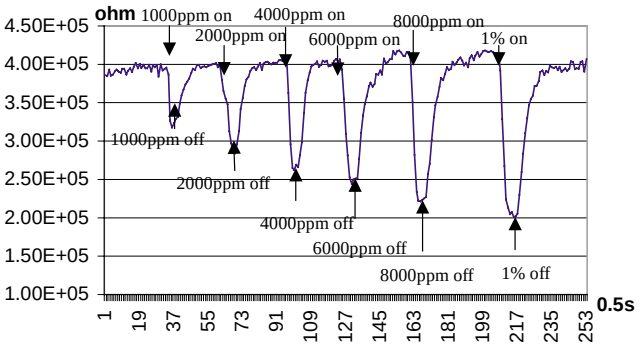

Fig. 11. Response of SnO_2 + 5% Ag + sputtered Pt to H_2 at 250 °C.

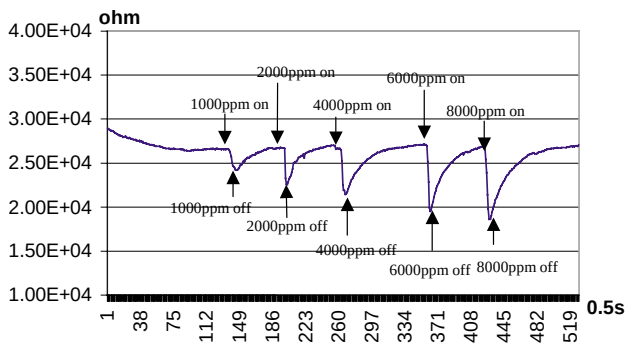

Fig. 12. Response of SnO_2 + 5% Ag + sputtered Pt to acetone at 300 °C.

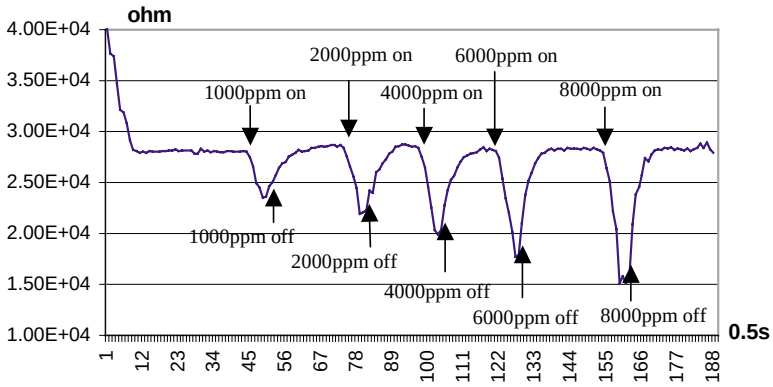

Fig. 13. Response of pure SnO_2 thin film ethanol at 300 °C.

sitivity gas sensors with nanocrystalline SnO_2 thin film attributes to two aspects. First, as particle size decreases, the surface to volume ratio increases largely (reverse proportional to the particle size), which leads to better sensitivity. According to the model brought up by Xu et al. [30], depending on the nanocrystalline size (D) relative to its space charge layer thickness (L), the transducer function is operated by a mechanism of grain-boundary control ($D \gg 2L$), neck control ($D > 2L$) or grain control ($D \leq 2L$), respectively. The gas sensitivity of nanocrystalline SnO_2 thin film is enhanced only when the film resistance is controlled by the latter two mechanisms, especially by the grain control mechanism. For the SnO_2 thin film, the space–charge layer thickness has been calculated to be ~3 nm at 250 °C [30]. As a result, the sensitivity increase steeply as D decreases and a maximum sensitivity can be achieved when the grain size is comparable with or less than $2L$ (≈6 nm for SnO_2). In the present study, the nanocrystalline SnO_2 particle size is less than 10 nm, prepared by the sol–gel process. This explains the enhanced sensitivity of this research.

Secondly, the porous topology of gas sensing thin film has great impact on gas sensing behavior. In this study, block copolymer as a convenient group of structure-directing agents, has been applied during the sol preparations. The mesoporous tin oxide thin film fabricated using this sol–gel process has large amount of film porosity, which also contribute to the enhanced sensitivity. Bai et al. [31] attribute this phenomenon to an enhanced Knudsen diffusion coefficient (D_k). For straight round pores within the thin film, D_k is given by

$$D_k = 9700r\left(\frac{T}{M}\right)^{1/2}$$

where, r is the pore radius, T the absolute temperature (K), and M the molecular weight of the gas for sensing. For a given film thickness, larger pore radius increases D_k, and hence would favor the improved gas concentration profile.

The thickness of nanocrystalline SnO_2 thin film is also important factor that greatly affect gas sensitivity. Unlike TiO_2, which is bulk conductance effects semiconductor, SnO_2 belong to the surface conductance effects semiconductors. The interaction between a semiconductor surface and H_2 (with reducing properties) can be explained in terms of reaction of hydrogen molecules with the pre-adsorbed oxygen:

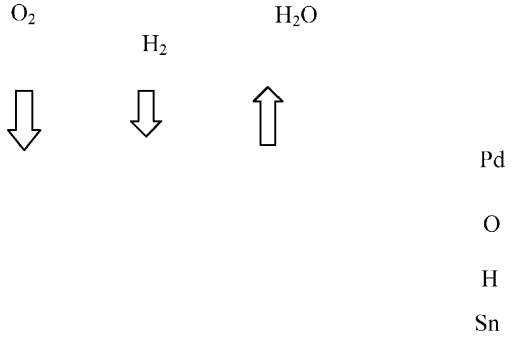

$$O_2^- + 2H_2\,(g) = 2H_2O\,(g) + e^- \quad (1)$$

$$O^- + H_2\,(g) = H_2O\,(g) + e^- \quad (2)$$

$$O_2^- + H_2\,(g) = H_2O\,(g) + 2e^- \quad (3)$$

Shukla and Seal [32] proposed that gas sensitivity of nanocrystalline SnO_2 thin film increases as decreasing the film thickness. However, below a critical film thickness of ~110 nm, the gas sensitivity decreases with further decrease

Table 4
Comparison of pure SnO_2 sensor response to acetone and ethanol at 300 °C

	1000 ppm	2000 ppm	4000 ppm	6000 ppm	8000 ppm	Response time	Recovery time
Acetone	8[a]	13[a]	18[a]	26[a]	36[a]	4 s	14 s
Ethanol	21[a]	27[a]	40[a]	55[a]	70[a]	3 s	9 s

[a] Values given in percentage.

in the film thickness. Very compact films exhibit lower surface areas and reduced Knudsen diffusion coefficient. As a result, they offer reduced number of active sites for the oxidation reactions with the reducing gases, and hence, would reduce the gas sensitivity with decreasing film thickness below this critical thickness range. In this investigation, the nanocrystalline SnO_2 film thickness is about 100–150 nm obtained via sol–gel spinning coating process under strictly controlled processing conditions.

From the testing results we also find that, as working temperature elevate, the resistance of gas sensing film decrease until reaches a stable level. Regarding to gas sensitivity, the SnO_2 has best sensitivity to hydrogen at 300 °C. This phenomenon can be explained: when operating temperature is below 300 °C (from room temperature to 300 °C), the desorption of water and adsorption of the oxygen-ions (O_2^- and O^- ions) dominates [31], which decreases the conduction electron density within the film, which favors the higher gas sensitivity [12], On the other hand, in the higher operating temperature range above 350 °C, the desorption of the oxygen-ions dominates. This thermally excites the electrons from the trap levels to the conduction band, which increases the conduction electron density, thus reducing the gas sensitivity [18,31]. SnO_2 has a broad range of sensibility to different chemical gases-based tested results in the research as well as reported in literatures. This character might cause cross sensitivity for a single sensor cell used in a gas mixture, but it is preferred for developing electronic nose system. Broad sensibility of SnO_2 means that a few sensing cells are need to detect a large number of chemical species with different dopants and catalysts. Pattern reorganization related data processing could be achieved by using ANN in the electronic nose.

4. Summary

MEMS-based sensor with doped nanocrystalline SnO_2 sensing films produce fast response time (2 s) and quick recovery time (10 s). The sensitivity to hydrogen at 100 ppm is good at 100 °C, even though 90% sensitivity can be achieved at 300 °C. Both doped with Pt and Ag has the similar performance, while sensor doped with Ag shows better performance, in terms of response time and sensitivity and more stabilized response. Good sensitivity of pure SnO_2 (without doping) nanofilm fabricated by sol–gel to different hydrocarbon (ethanol and acetone) has been achieved. The broad range of sensibility of SnO_2 to different chemical gases might cause cross sensitivity for a single sensor cell when it is used in a gas mixture, but this turns into an advantage for developing electronic nose system that a few sensing cells are need to detect a large number of chemical species. Pattern re-organization can be achieved by ANN. In future work, the sensor cell developed will be used for gas sensor array (different dopants and catalysts for specific gas) in an electronic nose in which fuzzy neural network will be applied for data processing and pattern reorganization.

Acknowledgements

The authors thank the partial support from UCF in-house grant for this research. The first two authors would also like to thank the partial support from Tyco Internationals Fire and Security.

References

[1] J. Chou, Hazardous Gas Monitors, McGraw-Hill, New York, 2000, ISBN 0-07-135876-5.
[2] http://www.epa.gov.
[3] F. Zee, J.W. Judy, Sens. Actuators B 72 (2001) 120–128.
[4] D.S. Lee, et al., Sens. Actuators B 71 (2000) 90–98.
[5] B.T. Marquis, J.F., Vetelino, Sens. Actuators B: Chemical, 77 (1–2, 15) (2001), 100–110.
[6] A.M. Pisanelli, et al., Life Chem. Rep. 11 (1994) 303–308.
[7] C.Y. Rebecca et al., Sens. Actuators B: Chemical, 93 (1–3, 1) (2000) 7–16.
[8] T. Nakamoto, et al., Sens. Actuators B 10 (1993) 85–90.
[9] J.E. Haugen, K. Kvaal, Meat. Sci. 49 (Suppl. 1) (1998) S273–S286.
[10] J.W. Gardner, K.C. Persaud, Electronic Noses and Olfaction, IOP Publishing Ltd., Bristol, 2000, ISBN 0-7503-0764-1.
[11] C.M. McEntegart, et al., Sens. Actuators B 70 (2000) 170–176.
[12] M. Penza, et al., Sens. Actuators B 81 (2001) 115–121.
[13] J.W. Gardner, Sens. Actuators B 4 (1991) 109–115.
[14] S.S. Park, J.D. Mackenzie, Thin Solid Films 274 (1996) 154–159.
[15] G. Sakai, et al., Sens. Actuators B 77 (2001) 116–121.
[16] I. Simon, et al., Sens. Actuators B 73 (2001) 1–26.
[17] G. Blaser, et al., Physics A 266 (1999) 218–223.
[18] J.W. Hammond, C.C. Liu, Sens. Actuators B 81 (2001) 25.
[19] Y. Lu, et al., Nature 389 (1997) 364.
[20] N.K. Raman, et al., Chem. Mater. 8 (1996) 1682.
[21] B.K. Miremadi, K. Colbow, Sens. Actuators B46 (1998) 30–34.
[22] S.P.S. Arya, et al., Thin Solid Films, 157 (1, 15) (1988) 169–174.
[23] T. Hyodo, et al., Sens. Actuators B 93 (2003) 590–600.
[24] Z.A. Ansari, et al., Sens. Actuators B 87 (2002) 105–114.
[25] P. Roland et al., Proceedings of the 2001 DOE Hydrogen Program review NREL/CP-570-30535, 2001.
[26] W. Gopel, K.D. Schierbaum, Sens. Actuators B 26–27 (1995) 1–12.
[27] K. Wada, M. Egashira, Sens. Actuators B 62 (2000) 211.
[28] M. Gaidi, et al., Sens. Actuators B 62 (2000) 43.
[29] S.G. Ansari, et al., Thin Solid Films 295 (1–2) (1997) 271–276.
[30] C. Xu, et al., Sens. Actuators B 3 (1991) 147.
[31] N.S. Bai, et al., Sens. Actuators B 63 (2000) 74.
[32] S. Shukla, S. Seal, Encyclopedia of Nanoscience and Nanotechnology, H.S. Nalwa (Ed.), American Scientific Publishers, Stevenson Ranch, CA, USA, 2003.

Biography

Dr. Quanfang Chen is currently an assistant professor and the program coordinator of Miniature Engineering Systems at the Mechani-

cal, Materials and Aerospace Engineering Department of University of Central Florida (UCF). He is also an affiliated faculty of Advanced Materials Processing and Analysis Center (AMPAC), and the director of MEMS Laboratory at UCF. Dr. Chen received his PhD from Tsinghua University in 1989. Before joining UCF, he was an assistant research professor (equivalent) at University of California at Los Angeles (UCLA). His research interests include microscale and nanoscale fabrications, multifunctional nanocomposite for MEMS/NEMS, sensors using nanostructural materials, actuators including hybrid compact actuators, microfluidic systems (valves and pumps) for Bio-MEMS, micro/nanomechanics including friction and control and molecular dynamic simulations.